

## WIND TURBINE AMPLITUDE MODULATION NOISE DUE TO TIME-DEPENDENT INTERFERENCE

Stuart Bradley

Physics Department, University of Auckland, Private Bag 92019, Auckland, New Zealand  
Email: s.bradley@auckland.ac.nz

### Abstract

Trailing edge noise from a turbine blade comprises sources which move in a circle so that the direct sound path and ground reflected sound paths to a receiver periodically vary. At any one listener location, there is therefore a fluctuating intensity. A simple ray model shows that this mechanism enhances the characteristics of wind turbine amplitude modulation noise, and can lead to a sharper onset of the higher intensity sound at some frequencies. This time-dependent interference mechanism does not depend on intermittent stall, although increased source intensity obviously leads to increased modulation noise.

### 1. Introduction

Particularly over the past decade noise from wind turbines has become a major concern for the public, and therefore for the industry. In addition to broad-band noise, generally identified as trailing edge noise, there has been an increasing concern about the annoyance to people by amplitude modulation (AM) of wind turbine noise [1]. A study by RenewableUK [2] provides wide cover of different aspects of AM and the more extreme version of modulation named “other amplitude modulation” (OAM). The main hypothesis for the cause of OAM in the RenewableUK study has been that it is due to intermittent stall of a blade. Oerlemans [3] developed a rotor simulation model including a noise model for a partially stalled airfoil and the model results showed the general observed characteristics of OAM. The source directivity characteristics of the stall noise are such that it is preferentially radiated upwind and downwind of the wind turbine and not in the cross wind direction as characterizes AM.

More recently, Madsen et al. [4] have correlated AM with turbine blade inflow conditions. They found a strong noise increase at low frequencies when a trailing edge stall initiates. For the turbine operating in a strong wind shear a modulation of the surface spectra for frequencies below 200Hz is 14dB. It was hypothesised that coupling with the turbine wake can cause abrupt changes in wind speed over the rotor disc and for a variable speed turbine the rotor might not be able to accelerate fast enough to avoid transient stall for a few revolutions. This intermittent occurrence might explain many of the occurrences of OAM.

The intermittent stall mechanism requires maintenance of stall conditions for a considerable time for the mechanism to be consistent with reported and observed OAM. Furthermore, the hypothesised wake coupling has yet to be verified with either a measurement program or via simulations. We have therefore in the current paper set out to explore an alternative, more continuously operating mechanism, “time-dependent interference”, to see if that might be plausible. This mechanism is based on the fact that, with three rotating blades and ground reflections, there are six possible sound paths to a fixed microphone position. For example, the images in Fig. 1 each show part of a single frame capture from the Norsonic 848 *Acoustic camera* [5]. The frequency band for these images is 1648 – 2630 Hz, these

high frequencies being used because of the small size of the acoustic camera. Note that the acoustic camera shows sound arriving at the microphone array from different directions, and does not combine the sound from various paths as a single microphone or ear would do. The left hand image shows sound reaching the camera from two blades. The central image shows sound being received from a direct path and from an indirect path ground reflection. The image on the right is from a further angular rotation of the blade by about 20° (0.3 s after the central image) and shows no ground reflection. Sound from the two sources identifiable in the left-hand image, or the two sources identifiable in the central image, reach the microphone array at the same time, but do not originate from the turbine at the same time because the path lengths to the array are different.

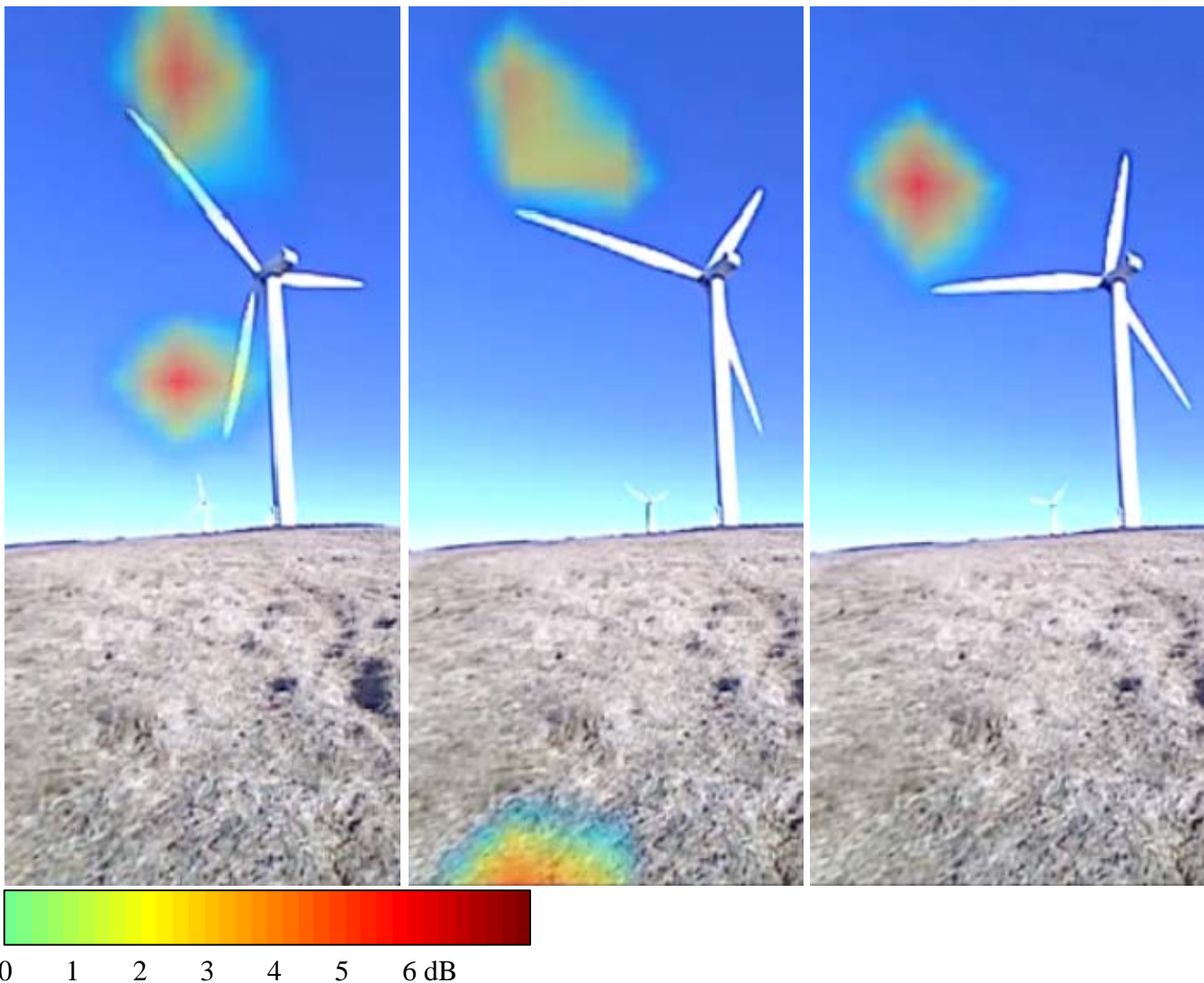


Figure 1. A single frame capture from a Norsonic 848 Acoustic camera showing sound originating from two blades.

The six pressure waves (a direct path and an indirect path from each of the three blades) originate at the turbine at different times and different blade positions. The combination of the six pressure waves therefore includes cancellations and reinforcements from the various amplitudes and phases as well as multiple frequencies from the six different Doppler shifted frequencies. The net result is to expect considerable modulation of the sound which would be emitted from a single blade.

It would appear that this mechanism has not been previously investigated, possibly because most effort has concentrated on the sound generation mechanisms on the rotor blades, and the sound propagation modelling has generally made use of conventional sound propagation codes which do not allow for multiple moving sources.



Two further angles are shown in Fig. 2 in connection with the direct path (similar angles can readily be defined for the indirect path). They are  $\beta$ , the angle at which the microphone is forward of the blade trailing edge (perpendicular to the rotor blade), and  $\varphi$ , the angle at which the microphone is lateral of the sound source (along the rotor blade). These angles are given in terms of other physical quantities by

$$\cos \varphi = -\hat{r}_d \cdot \hat{R} \quad (1)$$

(where the caret indicates a unit vector and  $\underline{R}$  is the radial vector from the hub along the blade to the noise source at the tip), and

$$\begin{aligned} \cos \beta &= -\hat{p} \cdot \hat{V} \\ &= -(\hat{r}_d + r_d \cos \varphi \hat{R}) \cdot \hat{V} \\ &= -\frac{\hat{r}_d \cdot \hat{V}}{\sin \varphi} \end{aligned} \quad (2)$$

The combined intensity dependence on trailing edge noise directivity and Doppler, or convective, amplification is [7]

$$\frac{\sin^2 \frac{\beta}{2} \sin \varphi}{(1 - M \hat{r}_d \cdot \hat{V})^4} = \frac{1}{2} \frac{\sin \varphi + \hat{r}_d \cdot \hat{V}}{(1 - M \hat{r}_d \cdot \hat{V})^4} \quad (3)$$

where  $M = V/c$  is the Mach number and the sound speed is  $c$ .

Ignoring for the moment the change in sound speed due to the wind, the direct path length,  $r_d$ , and indirect path length,  $r_i$ , are

$$\begin{aligned} r_d &= \sqrt{(d \cos \phi)^2 + (d \sin \phi + R \sin \alpha_d)^2 + (H + R \cos \alpha_d - h)^2} \\ r_i &= \sqrt{(d \cos \phi)^2 + (d \sin \phi + R \sin \alpha_i)^2 + (H + R \cos \alpha_i + h)^2} \end{aligned} \quad (4)$$

Sound emitted when a blade rotation angle is  $\alpha_d$  and  $\alpha_i$  reach the listener at time  $t$  where

$$\begin{aligned} \alpha_d &= \Omega \left( t - \frac{r_d}{c} \right) \\ \alpha_i &= \Omega \left( t - \frac{r_i}{c} \right) \end{aligned} \quad (5)$$

For each time  $t$  (4) and (5) need to be solved for  $r_d(t)$  and  $r_i(t)$ . Then the two intensities can be found from (3), and Doppler frequency shift values calculated. These parameters are all dependent on the geometry and the angular rotation rate of the turbine, but not on the sound source frequency spectrum. Once the path lengths are known as a function of time, the signals reaching the microphone can be combined with the correct phase for each emitted frequency  $f$ .

### 3. Selected results

For the following, the 2.3 MW turbine discussed in Chapter 3 of Bowdler and Leventhall [7] will be modelled. This has a rotor diameter  $D = 2R = 94$  m,  $H = D$ , and a typical value Mach number of  $M = 0.2$ . We consider a microphone at  $h = 1.5$  m, and use  $c = 340$  m s<sup>-1</sup>.

### 3.1 Locus of ground reflection point.

The point on the ground at which reflection occurs traces out an approximately (but not exactly) elliptical route for sound from each blade. These loci are shown in Fig. 3 for the cases of  $f = 315$  Hz,  $d = 2D$ , and  $\phi = 0^\circ$  and  $45^\circ$ . The closest approach of the reflection point to the microphone is when the sound originated from the top of the rotor sweep (note that acoustic camera images in Fig. 1 do not show the turbine blade and reflected sound synchronised). One useful item of information from this plot is that the ground reflection from such an elevated source is in general very close to the microphone (a distance of 2-6 m away for this case of  $d$  being 2 rotor diameters, and 4-12 m for  $d$  being 4 rotor diameters). This means that, for accurate sound propagation modelling, the ground impedance only needs to be known within a few meters of the microphone location.

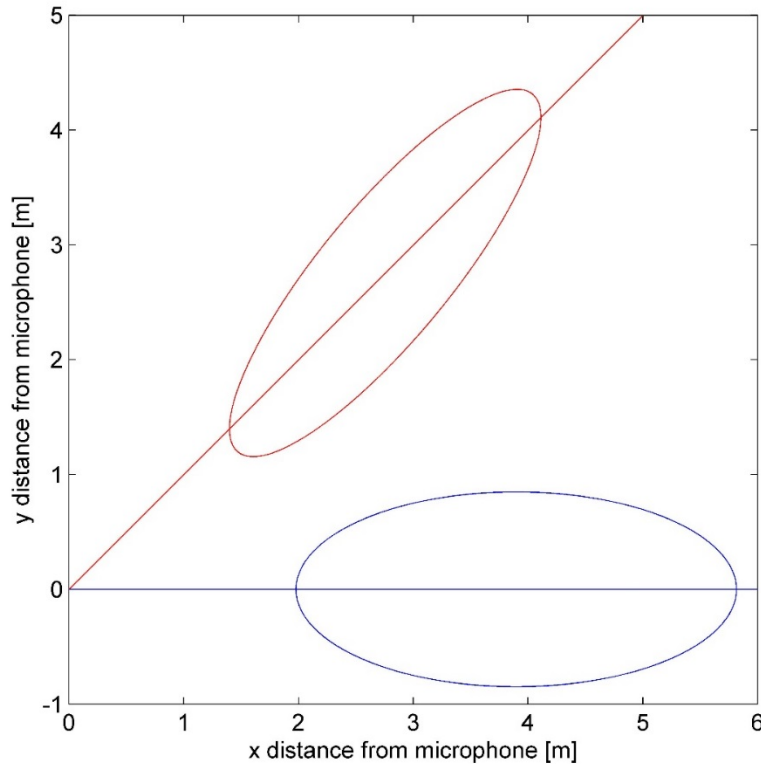


Figure 3. The approximately elliptical loci of ground reflection points for  $D = 94$  m,  $d = 2D$ ,  $H = D$ , and  $h = 1.5$  m, for  $\phi = 0^\circ$  (blue) and  $45^\circ$  (red). The straight lines are from the microphone location (shown here at the origin) toward the base of the turbine.

### 3.2 SPL from 1 blade, without considering Doppler frequency shift.

Fig. 4 shows the SPL due to noise from a single blade based on (3), as well as the combination of direct and indirect sound paths for a single blade, using the same parameter choice as in the previous section. In this figure the convective amplification is included, but not the effect on phase due to Doppler frequency shift. In this, and succeeding diagrams, the plots start at the time at which sound is received at the microphone from the top of the blade sweep i.e. there is a normalised delay of

$$\frac{\Omega \sqrt{d^2 + (H + R)^2}}{2\pi c}. \quad (6)$$

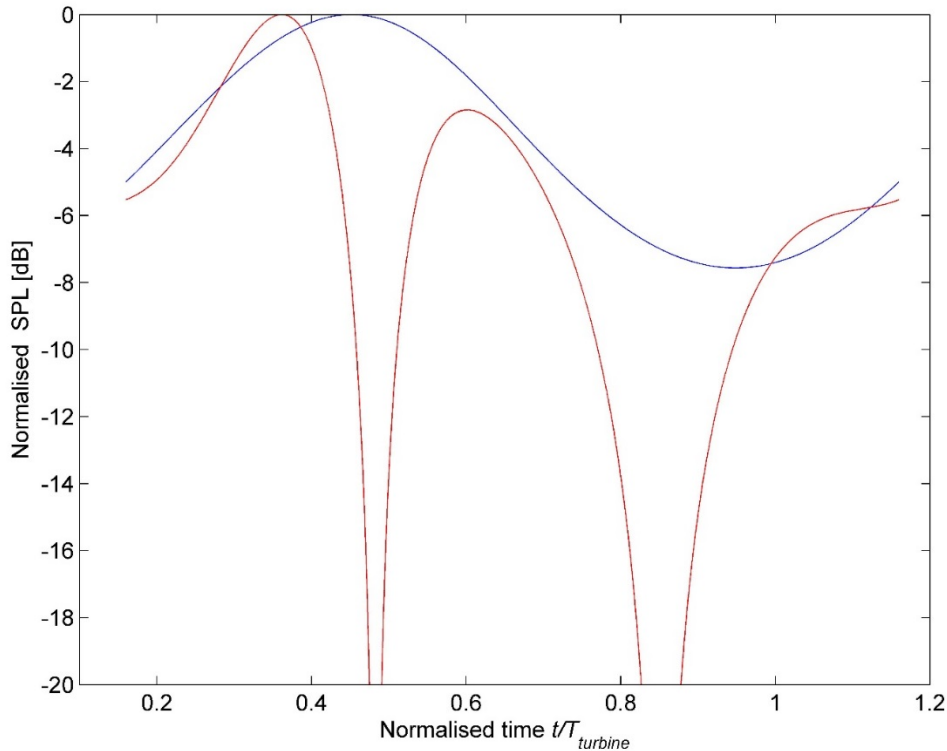


Figure 4. The SPL at the microphone for the direct path alone (blue) and for the combination of direct and indirect paths (red) from a single blade and a sound frequency of 315 Hz.

It can be seen that, for this sound frequency, the modulation of the received turbine noise is now around three times that of the rotation rate: if sound from the 3 blades were to be received independently there would be 9 intensity peaks during each rotation, or 3 intensity peaks per blade pass.

### 3.3 SPL from 1 blade and including Doppler frequency shift.

Fig. 5 shows, for the same parameter selection, the effect of including Doppler frequency shift on the combination of the direct and indirect path reception from a single blade. Some of the modulation features of Fig. 4 are preserved, but there is a lot more structure and higher modulation frequencies present due to the increased differences in frequency (and hence phase) of the sound in the direct and indirect paths. For this geometry and sound frequency, there is a modulation of around 10 times that of the blade pass rate. If the frequency is increased to  $f = 1$  kHz this modulation rate increases accordingly in proportion to  $f$  although, as in Fig. 5, the modulation is not uniformly sinusoidal.

Increasing the range from  $d = 2D$  to  $d = 4D$  makes the two paths shallower and the path differences smaller, with the result shown in Fig. 6. Shifting the microphone location from the downwind position by  $45^\circ$  (Fig. 7) changes where the minimum Doppler shift occurs on the blade rotation cycle. The combination of directivity and Doppler frequency differences with path causes a change in the modulation amplitude over the rotor cycle, but without changing the number of fluctuations per blade pass shown in Fig. 5.

### 3.4 SPL from 3 blades.

Fig. 8 shows the amplitude and Fig. 9 the spectrum of the received sound signal allowing for reception from the 6 paths and with Doppler frequency shifts.

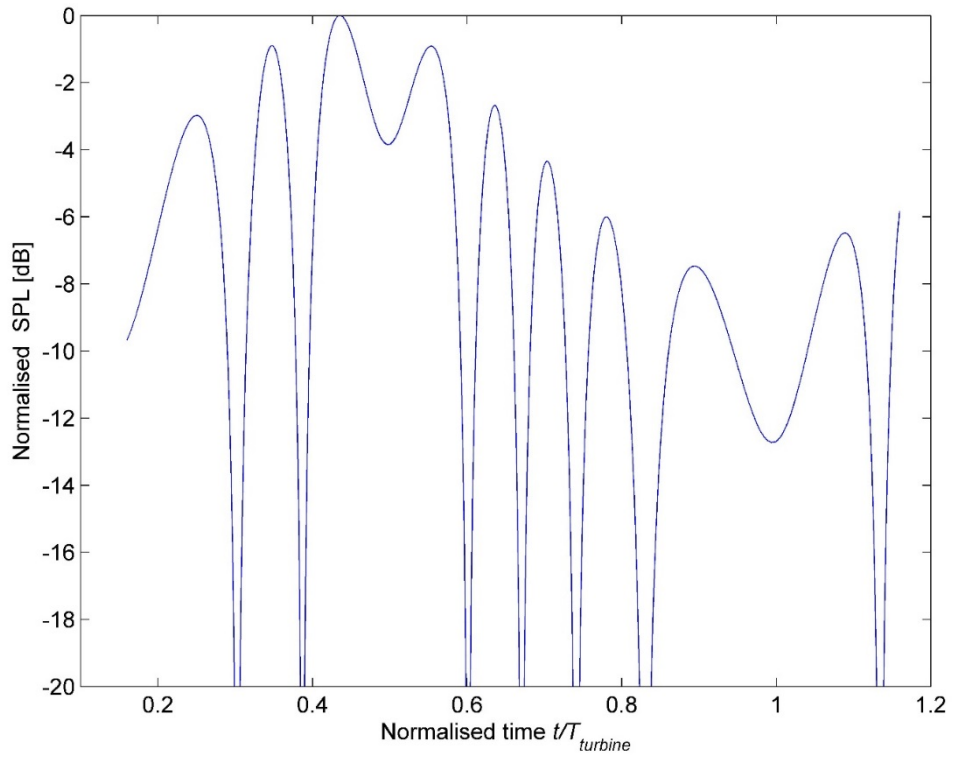


Figure 5. The SPL at the microphone from a single blade, including both direct and indirect paths, and the effect of Doppler frequency shift on phase.

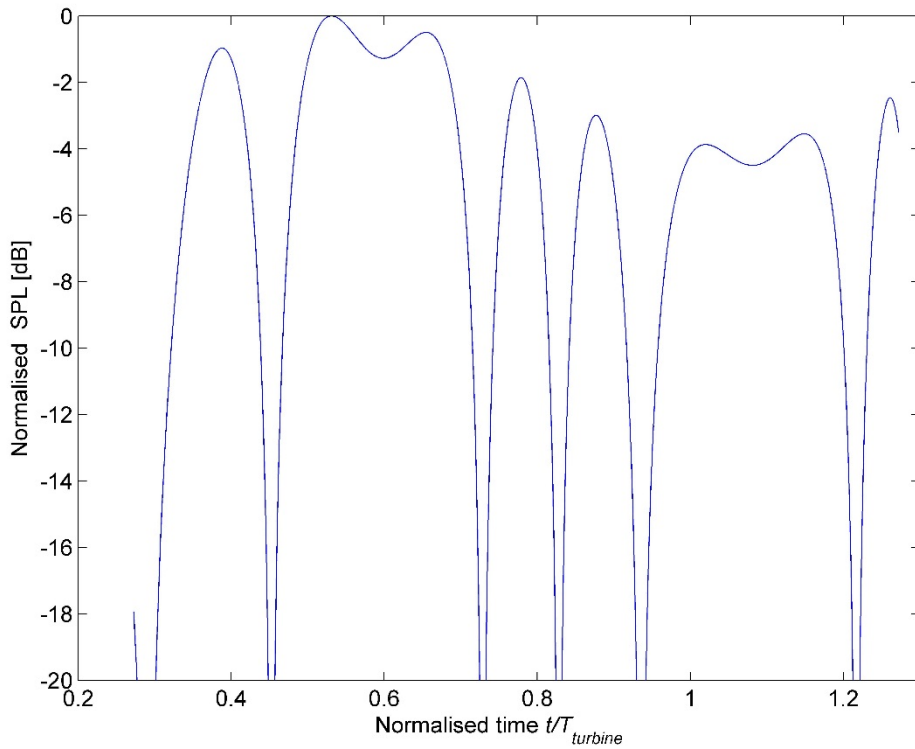


Figure 6. The SPL, as for Fig. 5 but with the range  $d = 4D$  instead of  $2D$ .

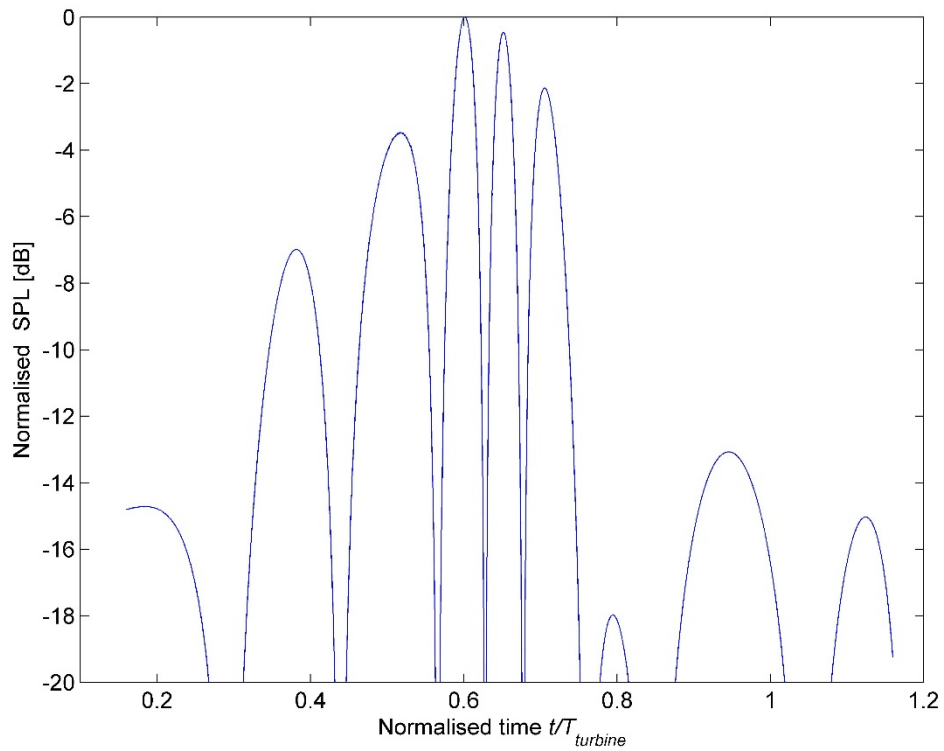


Figure 7. The SPL, as for Fig. 5 but with the range  $\phi = 45^\circ$  instead of  $0^\circ$ .

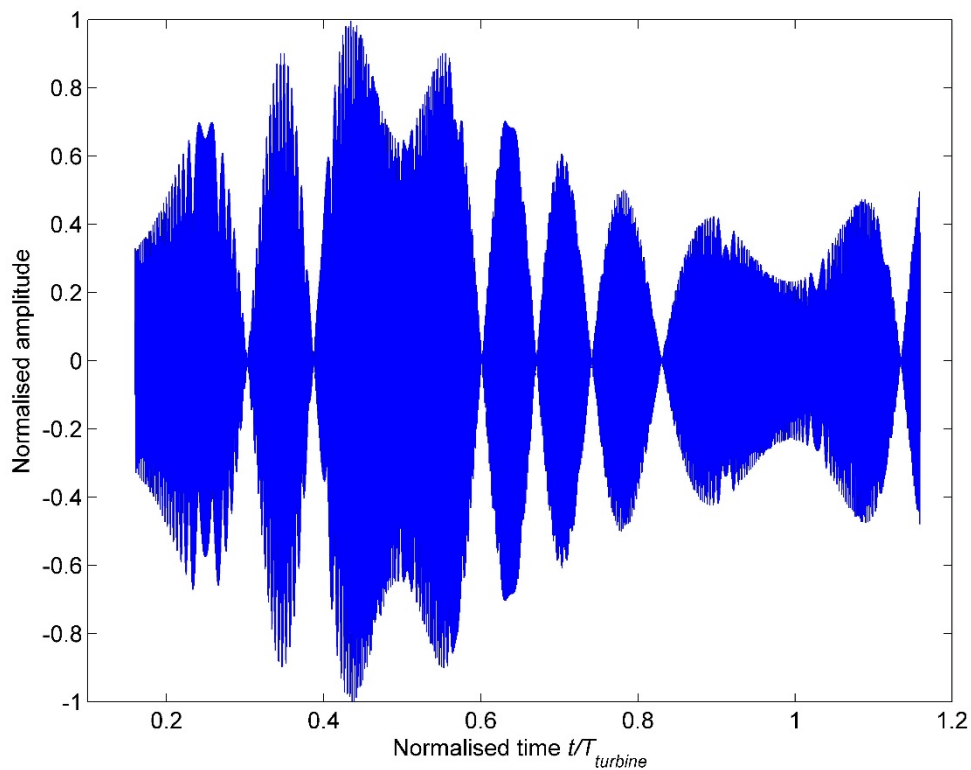


Figure 8. The received sound signal based on the parameters used in Fig. 4 and including the combination of Doppler-shifted signals from the 6 sound paths with appropriate time delays.

This sound displays strong amplitude modulation at all emitted frequencies. It is a continuous phenomenon. The spectrum, from this tonal emitted frequency, has finite bandwidth due to the maximum

and minimum Doppler frequency shifts defined by the geometry. Amplitude modulation of tonal signals, in radio for example, is achieved by adding structure in sidebands around the central frequency. This is what appears in Fig. 9. For this example geometry, at  $f = 315$  Hz, the bandwidth is limited to about  $\pm 100$  Hz, but the main amplitude fluctuations apparent in Fig. 8 have a frequency of only 2.4 Hz. The explanation for this difference lies in the time-varying nature of the Doppler shift which, in addition to AM, produces frequency modulation (FM). This means that, to understand the received sound, integration over the full emitted noise spectrum needs to be done since sound emitted in one 1/3-octave band will be received in another.

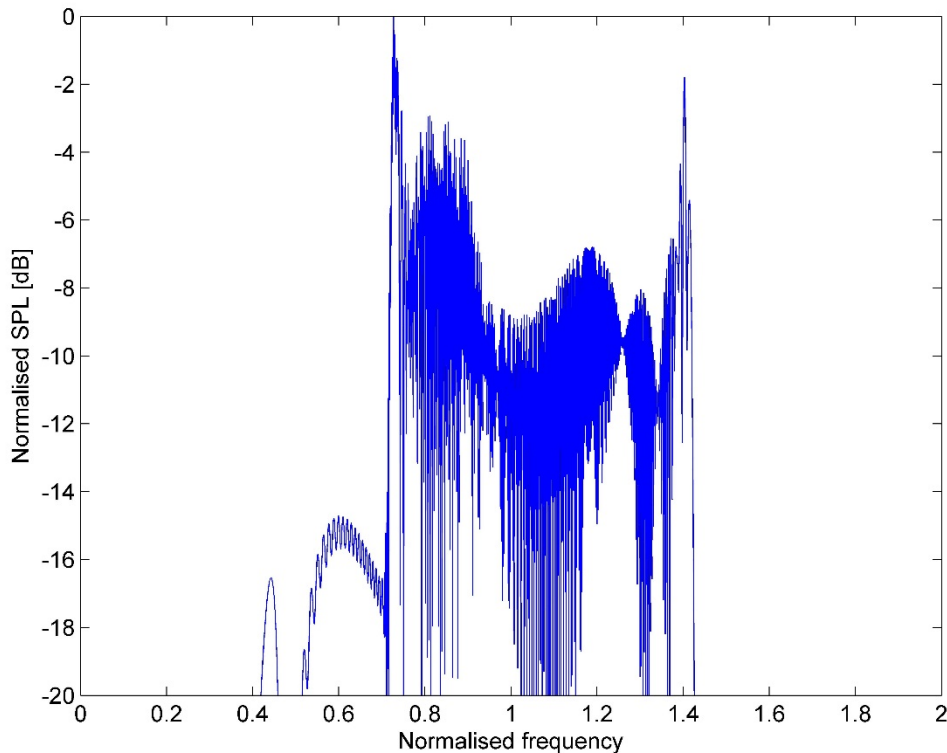


Figure 9. The spectrum of the received sound signal corresponding to Fig. 8.

#### 4. Refraction, Ground Impedance, and Full Spectrum

While we have not included here refraction, ground impedance, and integration over the full spectrum of emitted noise, these influences on propagation are not difficult to incorporate into our time-dependent interference model. In particular, curved propagation paths still require a numerical solution of equations like (4) and (5), allowing for the various propagation times from the 6 paths.

#### 5. Conclusions

In response to concern whether intermittent stall could account for sustained AM or OAM, we have suggested an alternative mechanism which is continuous in nature. This takes into account that sound reaching a receiver from multiple paths will have originated on the turbine blades at different blade positions. The result is that interference between sound travelling these different paths is much more dominant, and not static but changes during the turbine blade rotation cycle. This is a mechanism for modulation of the noise emitted from the turbine blade trailing edge.

For turbines the noise source is elevated and it is possible to show that only one ground reflection will occur for sound from a single blade and for typical geometries. For 3 blades this means that there are 6 paths for sound reaching a microphone. The interference between these 6 paths is strong and complex.

Simulations at discrete tonal emitted frequencies show classical amplitude modulation of the received signal, which is typically at a high multiple of the blade pass frequency. However, examination

of the spectrum shows a wider bandwidth than would account for the observed AM, because there is also FM arising from the more-or-less sinusoidally changing Doppler shifted frequencies received. Combining the full width of the emitted spectrum is likely to obscure this FM component while still retaining the strong AM nature.

While investigation of this mechanism is ongoing, it is clear from the simulations shown here that many of the observed characteristics of AM and OAM are reproduced, including the reduction in modulation frequency if the microphone is moved away from the downwind or upwind direction. Interestingly, a good way for distinguishing intermittent stall from time-dependent interference, would be to use an acoustic camera. This is a strong motivation for the DTU design of a Large Aperture Acoustic Camera (LAAC), which is discussed in another paper at this conference.

## References

- [1] Bowdler, D. Amplitude modulation of wind turbine noise: a review of the evidence. *Institute of Acoustics Bulletin*, 33, 31–41, 2008.
- [2] Bullmore, A., M. Cand, S. Oerlemans, M. Smith, P. White, S. von Hünenbein, A. King, and B. Piper. *Wind Turbine Amplitude Modulation: Research to Improve Understanding as to its Cause and Effects*. RUK, <http://www.renewableuk.com/en/publications/index.cfm/wind-turbine-amplitude-modulation>, 2013
- [3] Oerlemans, S. An explanation for enhanced amplitude modulation of wind turbine noise. In *RenewableUK 2013 report: Wind Turbine Amplitude Modulation: Research to Improve Understanding as to its Cause & Effect*, 2013
- [4] Madsen, H. A., F. Bertagnolio, A. Fischer, and C. Bak Correlation of amplitude modulation to inflow characteristics. *INTER-NOISE and NOISE-CON Congress and Conference Proceedings*, Vol. 249 of, 12136–12136, 2014
- [5] 4Dnoise, 2104: Norsonic video. <http://4dnoise.com/2014/01/04/visualising-wind-turbine-noise-using-acoustic-camera-and-listen/> (Accessed 2014).
- [6] Salomons, E. M. *Computational atmospheric acoustics*. Springer Science & Business Media, 2001
- [7] Bowdler, D., and G. Leventhall *Wind Turbine Noise*. Bowdler, Dick and Leventhall, Geoff, Ed. Multi-Science Publishing, 2011